The Pre-storm Environment of Midlatitude Prefrontal Squall Lines

JONATHAN WYSS AND KERRY A. EMANUEL

Center for Meteorology and Physical Oceanography, Massachusetts Institute of Technology, Cambridge, Massachusetts

28 April 1987 and 28 August 1987

ABSTRACT

Composite environmental profiles of wind and temperature are presented for squall line cases that are spatially removed from frontal disturbances. The motions of the squall lines are inferred from radar data, and the mean environmental wind profile is presented in a coordinate system relative to the squall line. The dataset consists of 60 cases from all seasons and from various geographical regions of the continental United States. The results are compared to a similar study by Bluestein and Jain.

1. Introduction

Squall lines, traditionally labeled as midlatitude or tropical according to their origins, are characterized by deep convection, strong surface winds, and intense precipitation. Perhaps most intriguing is the apparent autonomous nature of such storms: numerous studies, since Newton (1950), have remarked on the wide range of directions and speeds at which squall lines are observed to propagate.

Although several case studies of extratropical squall lines have been published (e.g., Fujita, 1955; Ogura and Liou, 1980), no climatologies are available, with the exception of Bluestein and Jain (1985), who investigated severe squall lines occurring in Oklahoma during the spring. In this study, which considers prefrontal squall lines occurring over the entire continental United States, no limitations were introduced regarding the strength of the convection, or the season. However, only convective lines distinct from nearby frontal systems were included, in an attempt to determine which characteristics of the atmospheric environment might be necessary, or sufficient, for squall line formation and propagation.

Composite soundings and wind profiles of the pre-storm environment are presented. Such climatological mean profiles could be useful for specifying realistic initial conditions in numerical modeling studies.

2. Data

Of the approximately two hundred squall line occurrences reported on National Weather Service (NWS) surface analyses and radar summaries between June 1981 and November 1983, 60 cases were considered in this study (Table 1). This subset was selected on the basis of the following criteria: distinct spatial separation between the squall line and any associated cold front; persistence of the squall line over several hours; quasi-steady intensity, velocity, and areal extent of the storm in time; and local availability of radar summaries, NWS analyses, and an upper air sounding ahead of the squall line. All of the squall lines selected are cases where the convection associated with the line is well separated from any convection along the front. None of the cases developed along the front, propagating ahead, nor were they later overtaken by the front while still active lines.

The velocity of each squall line was determined from NWS radar summaries. Successive tracings of the storm outline, as depicted by the VIP reflectivity contours on the hourly maps, were superimposed, and the speed of the squall system measured as the mean rate of translation of the major axis of the storm. The position of the major axis was arbitrarily defined as the leading edge of the VIP level 3 reflectivity contour (41 dBZ). The accuracy of estimation of the squall line velocity is limited by the quality of the radar summaries. Comparisons of the summaries with archived MIT radar data for New England storms yielded errors in the determination of the line speed between 1 and 5 m s^{-1}.

Wind, temperature, and moisture characteristics of the pre-storm environment were determined both from upper air soundings and from NWS standard pressure level analyses. Single soundings were chosen as being representative of the environment through which the squall line ultimately progressed, and geostrophic analyses of height fields were performed at standard pressure levels.

3. Squall line characteristics

All of the squall line cases considered in this study occurred east of the Rocky Mountains: 18 formed in

Corresponding author address: Jonathan Wyss, Center for Meteorology and Physical Oceanography, MIT Room 54-1711, Cambridge, MA 02139.

TABLE 1. Dates (day/month/year) and locations of squall lines considered in study.

1	Nebraska	2/8/81	31	Alabama	27/12/82
2	Georgia	11/8/81	32	Texas	9/2/83
3	Alabama	16/4/82	33	Alabama	5/3/83
4	Arkansas	17/4/82	34	Alabama	2/4/83
5	Georgia	17/4/82	35	Ohio	2/5/83
6	Texas	6/5/82	36	Texas	10/5/83
7	Oklahoma	15/5/82	37	Texas	11/5/83
8	Oklahoma	17/5/82	38	Indiana	14/5/83
9	Texas	17/5/82	39	Oklahoma	14/5/83
10	Texas	24/5/82	40	Oklahoma	14/5/83
11	Mississippi	25/5/82	41	North Carolina	17/5/83
12	Missouri	29/5/82	42	Louisiana	19/5/83
13	Mississippi	31/5/82	43	Alabama	22/5/83
14	North Carolina	31/5/82	44	Louisiana	22/5/83
15	Oklahoma	11/6/82	45	Louisiana	22/5/83
16	Georgia	12/6/82	46	Kentucky	22/5/83
17	Alabama	13/6/82	47	Georgia	22/5/83
18	Texas	24/6/82	48	Florida	23/5/83
19	North Carolina	3/7/82	49	Missouri	29/5/83
20	Wisconsin	7/7/82	50	Ohio	29/5/83
21	Colorado	15/7/82	51	Tennessee	4/6/83
22	Nebraska	15/7/82	52	Oklahoma	28/6/83
23	Iowa	17/7/82	53	Oklahoma	6/28/83
24	Pennsylvania	18/7/82	54	Arkansas	29/6/83
25	Ohio	18/7/82	55	Arkansas	2/7/83
26	Mississippi	2/9/82	56	Tennessee	2/8/83
27	Pennsylvania	3/9/82	57	Oklahoma	13/9/83
28	Missouri	14/9/82	58	Tennessee	4/10/83
29	Arkansas	2/11/82	59	Pennsylvania	5/10/83
30	Alabama	12/11/82	60	Arkansas	2/11/83

the south-central states; 13 in the Midwest; and 29 in the Southeast. Cases from all months are represented in the sample, although late spring was the period of most frequent occurrence. Prefrontal convective lines during the winter months were most frequently located in Florida and along the Gulf Coast; in the Plains states during late spring and early summer; and in the Midwest and Northeast during late summer and fall.

The locations of the squall lines relative to the synoptic system varied from case to case, adopting any orientation with respect to the frontal system. In general though, the lines were roughly parallel to the cold front. The distance between the squall lines and the nearest cold front ranged from 100 to 700 km. The direction of squall line motion (perpendicular to the major axis of the line in all cases), was most frequently towards the southeast (mean 130 deg; σ = 30 deg). The translational velocities of the squall lines, as determined from the radar summaries, ranged from 1 to 20 m s^{-1} (mean 10 m s^{-1}; σ = 4 m s^{-1}).

The areal extent of the radar echoes varied considerably between cases, although within a storm, during the period of development for which velocities were calculated, the morphology of the storm did not change appreciably. The average length of the squall lines, defined by the VIP level 3 contour, was 330 km, with a length/width ratio greater than five.

4. Pre-storm environment

Composite thermodynamic and wind profiles were obtained in an attempt to determine which characteristics of the environment are conducive to squall line development and how they might affect the direction and speed of propagation. Attempts to stratify the data according to the aforementioned geographic regions did not produce significant differences in the mean profiles.

Averaged temperature and humidity profiles compiled from the soundings exhibit a local minimum in the mixing ratio between 650 and 500 mb, with a corresponding minimum in the equivalent potential temperature near 600 mb. Mean profiles of the equivalent potential temperature (θ_e) and saturation equivalent potential temperature (θ_e^*), calculated from the mean temperature and dew-point profiles for the sixty cases, are presented in Fig. 1. Plotting the sounding in terms of θ_e and θ_e^* emphasizes the mean degree of conditional instability in the pre-storm environment. The composite profile is conditionally unstable to parcels lifted from below 800 mb.

Calculations of convective available potential energy (CAPE) and of convective inhibition (CIN) were made for 36 of the 60 soundings. This subset does not include data from 1200 UTC soundings, in which the mixed

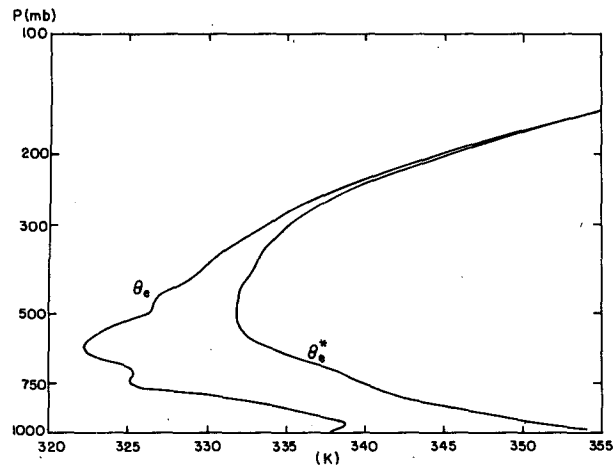

FIG. 1. Vertical profiles of equivalent potential temperature (θ_e), and saturated potential temperature (θ_e^*). Calculated from averaged soundings of sixty squall line cases.

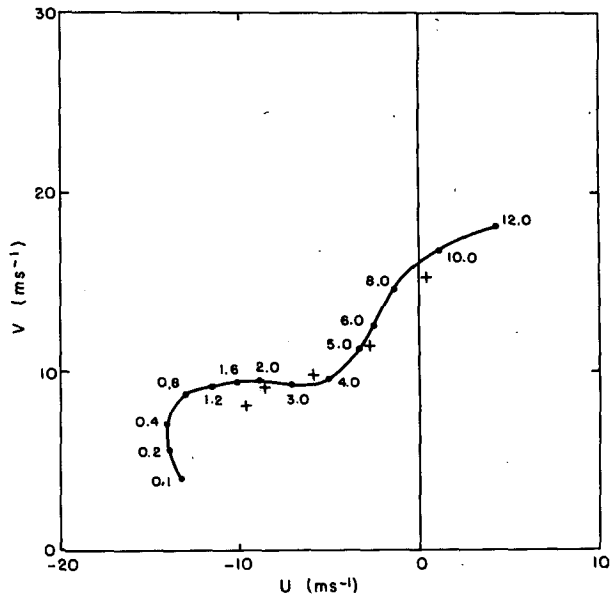

FIG. 2a. Hodograph in squall line relative coordinates. Values along solid line are heights (km MSL). Crosses define corresponding hodograph for geostrophic winds derived from height analyses at standard pressure levels (surface, 850, 700, 500 and 300 mb).

layer was not well established. The calculations were performed assuming parcel potential temperature and mixing ratio equal to averages over the lowest 500 m; pseudo-adiabats and integrations were computed numerically, following Bolton (1980) and Stackpole (1967).

Average values of CAPE and CIN are 1208 (1121) and 76 (88) respectively, in units of $m^2 s^{-2}$, with standard deviations in parentheses. Corresponding values from Bluestein and Jain (1985) are 2260 (1100) and 33 (83), which are comparable to values for several of the more severe squall line cases included in this study. The CAPE and CIN for the composite sounding of Fig. 1 are 660 and 83 respectively. Attempts to distinguish between severe and less severe cases on the basis of CAPE yielded no significant differences in the mean velocity or other characteristics of the lines. Moreover, the frequency distribution of CAPE for the 36 cases indicates no signs of bimodality.

Characteristics of the ambient wind field will be examined with respect to a reference frame moving with the squall line. The coordinate system is defined such that the y-axis is aligned with the major axis of the squall line. With these conventions, the u component of velocity represents relative flow across the line in the direction of squall line motion, while the v component corresponds to flow along the line. Negative u implies that the squall line is moving faster than the environmental winds at a given level, and $u = 0$ represents a steering level with respect to the propagation of the line.

The hodograph in Fig. 2a represents the composite vertical profile of relative velocity, as derived from the sounding data. Depicting the profile in this manner has the advantage of emphasizing the orientation of the squall line relative to the shear, since the shear vector is everywhere tangent to the hodograph curve. Also plotted is the corresponding mean hodograph derived from geostrophic wind analyses at standard pressure levels (crosses). At upper levels, the geostrophic winds provide a good estimate of the mean ambient wind field, unperturbed by the squall line itself. Figure 2b is

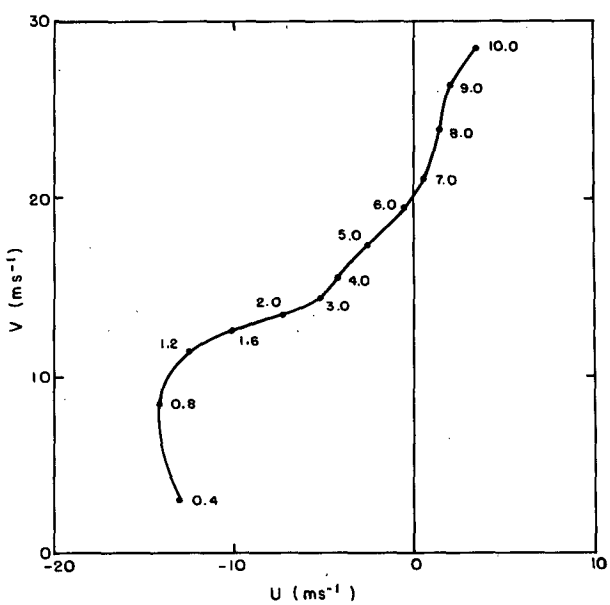

FIG. 2b. As in Fig. 2a but from Bluestein and Jain (1985), for severe Oklahoma squall lines in the spring.

reproduced from Bluestein and Jain (1985) for comparison.

The essential features of the two hodographs are strikingly similar, although the Oklahoma storms exhibit a larger component of velocity along the line, marginally stronger shear throughout the troposphere, and a lower mean steering level.

In broad agreement with Bluestein and Jain (1985), the squall lines are oriented along the shear in the lowest 1 km; nearly perpendicular to the shear between 1 and 3 km; and at an angle of roughly 45 deg above 3 km. Similar results were obtained when the shear of the geostrophic wind was considered for individual cases. The modes of the distributions of the differences between the line orientation and the shear vectors are as follows: SFC–850 mb, 30 deg; 850–700 mb, 90 deg; 700–500 mb, 70 deg; 500–300 mb, 60 deg.

Figure 3 depicts the vertical variation of the standard deviations of the u and v components. There is an increase in the variance with height, due in part to instrument error. More significant is the observation that the deviations are greatest for the component of velocity along the line, at nearly all levels. This supports the notion that the dynamics of the squall line are in a gross sense two dimensional; less sensitive to variations along the line than to variations in the cross-line direction. Also, again in agreement with Bluestein and Jain (1985), there is a pronounced maximum in σ_u near cloud base, in the region where the hodograph is sharply curved.

With regard to steering levels for the motion ($u = 0$), Fig. 2a suggests that such levels exist only near 9 km, (compared to 6 km in Fig. 2b). However, the frequency distribution of the height of occurrence of steering levels exhibits a significant maximum between 4 and 6 km, and lesser maxima at 9 and 11 km. Eighty-three percent of the cases contained steering levels at some height below the tropopause.

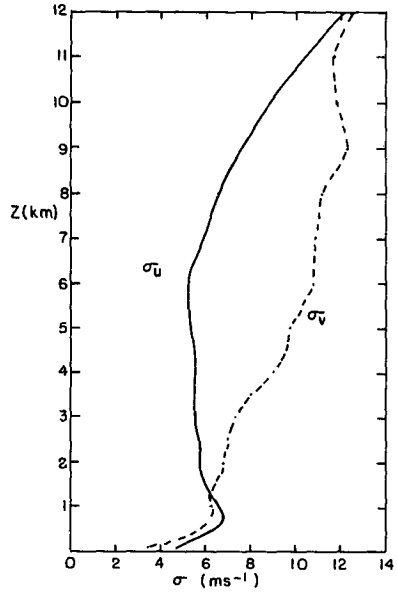

FIG. 3. Vertical variation of standard deviations of relative velocity components: cross-line (u, solid); along-line (v, dashed).

5. Concluding remarks

Various parameters, derived from the thermodynamic and wind fields, were examined as predictors of squall line movement. Linear correlations of the squall line speed with the cross-line component of the environmental flow at standard pressure levels yielded low correlations. The best linear fits occurred at the 500 and 700 mb levels, with correlation coefficients close to 0.5 (95% confidence limits ± 0.2). 90% of the lines moved faster than the cross-line component of the wind at 700 mb.

Attempts were also made to correlate the observed squall line speeds with various theoretical predictions. In particular, the hypothesis that the speed of propagation is proportional to the speed of a gust front generated by evaporatively cooled downdraughts (Charba, 1974) was tested. The negative buoyancy of the density current was calculated for evaporatively cooled subcloud air, and for parcels descending from midtropospheric levels where the potential wet-bulb temperature reaches a minimum. The predictions of Moncrieff and Miller (1976), derived for squall lines in a low shear regime where the speed of propagation is proportional to the square root of CAPE, were also analysed. None of these correlations with the data was significant (at the 95% level). These results are inconclusive because of both the large errors associated with the determination of the squall line speeds from the radar maps, and the crude assumptions introduced in the calculation of the predicted speeds. On the other hand, the effects of such error are significantly reduced by the process of averaging to produce a climatology of the squall line environment.

Many of the salient features of the Bluestein and Jain (1985) climatology are also evident in this study, indicating that these are characteristic of the pre-storm environment of a wider class of squall lines: cases of varying severity, from different geographical regions, occurring in all seasons. Numerical simulations of squall lines will benefit from the availability of mean profiles of wind, temperature, and moisture as presented both in Bluestein and Jain (1985) and in this study. It should be remembered, however, that soundings should be selected which contain both the characteristics embodied in the composite profiles, and the mean characteristics of the sample, such as CAPE and the mean steering level for the motion, which are not necessarily expressed in the composite profiles.

Acknowledgments. This research was partially supported by NSF Grant ATM-8313454.

REFERENCES

Bluestein, H. B., and M. H. Jain, 1985: Formation of mesoscale lines of precipitation: severe squall lines in Oklahoma during the spring. *J. Atmos. Sci.*, **42,** 1711–1732.

Bolton, D., 1980: The computation of equivalent potential temperature. *Mon. Wea. Rev.*, **108,** 1046–1053.

Charba, J., 1974: Application of gravity current model to analysis of squall line gust front. *Mon. Wea. Rev.*, **102,** 140–156.

Fujita, T., 1955: Results of detailed synoptic studies of squall lines. *Tellus,* **7,** 405–436.

Moncrieff, M. W., and M. J. Miller, 1976: The dynamics and simulation of tropical cumulonimbus and squall lines. *Quart. J. Roy. Met. Soc.*, **102,** 373–394.

Newton, C. W., 1950: Structure and mechanism of the pre-frontal squalls. *J. Meteor.*, **7,** 210–222.

Ogura, Y., and M. Liou, 1980: The structure of a midlatitude squall line. *J. Atmos. Sci.*, **37,** 553–567.

Stackpole, J. K., 1967: Numerical analysis of atmospheric sounding. *J. Appl. Meteor.*, **6,** 464–467.